PAPER • OPEN ACCESS

Comparative H diffusion measurement through metal and non-metal nano-layers using optical sensing

Comparative H diffusion measurement through metal and non-metal nano-layers using optical sensing

O Soroka[1], J M Sturm[1] , C J Lee[2] and F Bijkerk[1]

[1] Industrial Focus Group XUV Optics, MESA+ Institute for Nanotechnology, University of Twente, P.O. Box 217, 7500 AE, Enschede, The Netherlands
[2] Fontys Institute of Engineering, De Rondom 1, 5612 AP, Eindhoven, The Netherlands

E-mail: j.m.sturm@utwente.nl

CrossMark

Abstract

In this work, a technique for hydrogen diffusion measurements through thin films is proposed and demonstrated. A yttrium film, which changes its refractive index upon hydrogen absorption, is used as an optical sensor to detect hydrogen. The yttrium sensor is coated with a thin (up to 12 nm) layer of test material and exposed to atomic hydrogen. To ensure that the calculated diffusion constant is not artificially changed by surfaces processes, the test layer is coated with palladium. Hydrogen diffusion through test layers of Si, Al, Ag, Ru, Mo, Al_2O_3 and SiO_2 were measured and compared with existing data. The hydrogenation time (time to form YH_2) was found to exponentially scale with the enthalpy of hydrogen solution in the test material. Comparison between measured diffusion coefficients for different film thicknesses, as well as previously reported results, highlights the strong dependence of the diffusion constant on sample fabrication conditions, and hydrogen exposure conditions. It is concluded that diffusion through thin films can be reliably compared only when specimen form and exposure conditions are the same. The relevance of this study for applications is discussed.

Keywords: hydrogen diffusion, thin films, ellipsometry, yttrium, YH_2

Some figures may appear in colour only in the online journal

1. Introduction

Understanding the interactions between hydrogen and solids has been a focus of many studies. Interest in this topic has been motivated by the high susceptibility of many materials to hydrogen containing environments. Furthermore, uptake of hydrogen can induce changes in material properties, such as conductivity and durability. This is due to the small size of the hydrogen atom that allows its fast diffusion into the bulk of materials, and the high reactivity of hydrogen with metals and other materials.

Studies of hydrogen interactions with solid materials span decades and a large variety of measurement techniques have been employed, depending on measured parameters and type of sample under investigation. To measure the hydrogen concentration absorbed by a material, techniques such as volumetric and mass difference measurements, nuclear reaction analysis and elastic recoil detection analysis have been employed [1]. For the measurement of H mobility, permeation measurements [2, 3], and optical techniques like hydrogenography [4] are often used. However, the measured parameters may have different definitions, depending on both the chosen method, and the size and shape of the specimen. Indeed, a wide variety of solid materials have been investigated, including powders, micrometer-thick membranes, wires, tubes, and nanometer-thick thin films, which makes a direct comparison between the hydrogen mobilities or concentrations obtained from different studies unreliable.

Hydrogen uptake by and mobility in thin films is not the same as in a bulk sample due to structural differences, making comparison (direct or indirect) between experimental results extremely challenging. Yet, knowledge of hydrogen permeability through micro- and nanometer-thick layers is essential for hydrogen barrier applications. Shielding materials for hydrogen is relevant to applications such as nuclear fusion reactors [5], extreme ultraviolet lithography [6, 7] and space engineering, since uptake of hydrogen can lead to, for example, hydrogen embrittlement [8] or blister formation [9]. It is, therefore, highly desirable to develop a method that makes a direct comparison between hydrogen permeation through thin films of different materials possible.

Optical sensors are often used to measure the uptake of hydrogen. Optical sensors offer safe integration into hydrogen environments, since they do not need electrical contacts to the sample under investigation, as would be the case with resistivity methods. In addition, optical measurements are easily accessible, straightforward to apply *in situ*, and can be used over a wider pressure range, as opposed to ion beam methods [10].

In this work, we demonstrate an effective method for comparing the hydrogen transport through thin films of different materials. The hydrogen permeation through test layers of Ag, Al, Si, Ru, Mo, Cu, SiO_2 and Al_2O_3 was studied using a Y sensor layer. Diffusion constants are obtained for several samples, which show that for many ultrathin films, the diffusion constant is strongly dependent on the film thickness. By comparing the tabulated heat of dissolution with the time it takes to saturate the Y layer, it is possible to qualitatively determine the relative contribution between dissolution and other diffusive mechanisms. By comparing the hydrogenation rates, the limiting processes for hydrogen transport are discussed. This work builds upon previous work in our group on studying the interaction of hydrogen with thin film materials, using a Y sensor layer. The knowledge on the influence of the surface material properties on H uptake kinetics [11] allowed a sample structure to be designed, and exposure conditions chosen, for which diffusion through the test layer limits the overall hydrogenation rate, as detailed in section 2. Together with our previous calibration of ellipsometry signatures of different Y hydride phases [12], this allowed us to study diffusion through a larger set of materials and compare these results to literature data and our previous publication on H diffusion through Ru [13].

2. Sensor model

Some metals show large changes in optical properties upon hydride formation, which makes them good candidates as a hydrogen sensor [14, 15]. For instance, Y forms di- and trihydride upon exposure to hydrogen, which can be readily detected optically with, for example, ellipsometry or transmission measurements. When depositing a test layer of material under investigation on a Y film, it is possible, provided that

the layer stack and exposure conditions are properly chosen, to relate the measured hydrogenation rate of Y to hydrogen diffusivity through the test layer. Effectively, to obtain the diffusivity of the test layer and to compare diffusion constants, the layer stack must be chosen such that differences in surface processes are eliminated [11, 16], that the flux through the sample surface is known, and that the diffusion through the test layer is slow compared to diffusion through all other layers in the stack [13]. The results below indicate that these conditions may be readily met for a wide range of materials.

Previous studies on hydrogenation kinetics of Y films with a protective or catalytic capping layer showed that the hydrogenation process may be limited by surface processes on the capping layer, bulk diffusion processes, or interface processes [16, 17]. Surface processes may even determine which hydride forms. For instance, a Ru cap leads to the formation of YH_3, while a Ag cap prevents any measurable hydrogenation [11]. To eliminate the difference in ad- and desorption kinetics of hydrogen for each material and its influence on the saturation level of the Y layer with hydrogen [11], a palladium capping layer is added on top of the test layer to promote hydrogen adsorption and make the influence of the surface processes equal for all test layer materials. In this way, as was proposed in prior work [13], the transport of hydrogen through test layers can be studied and compared for different materials. In addition, the use of Pd capping layer in so-called switchable Y mirrors has been demonstrated in a prior study [18].

In order to obtain the diffusivity, the flux of (atomic) hydrogen through the test layer must be known. In most research, the sample is subjected to a known molecular hydrogen pressure, which requires that the influence of the H_2 chemisorption and dissociation on the measured hydrogenation rate should be taken into account in order to calculate the flux. To eliminate the influence of dissociation, we expose test samples to atomic H. Atomic H also has a higher sticking probability than H_2, which allows saturated surface coverage to be reached at low hydrogen pressures, thereby reducing the role of surface processes on the overall hydrogen diffusion rate through the stack. The experimental evidence of the accelerated diffusion rate when using an atomic hydrogen source in combination with a Pd cap is shown further in the Results and discussion section (see figures 2 and 3).

Pd has a large hydrogen diffusion constant and (in comparison to other metals) absorbs hydrogen rapidly [19]. Provided that the test materials have a lower diffusion constant than Pd, the combination of atomic hydrogen and Pd ensures that all test materials, denoted as Ma, will be exposed to the same (relatively high) hydrogen concentration at the Pd/Ma interface. Thus, by creating samples that have the same surface (Pd in our case) and ensuring that the top Pd layer is saturated, then the hydrogenation rate of the sensor film can be associated with hydrogen permeation through the test layer. This has the additional advantage of working at hydrogen pressures that are compatible with (ultra) high vacuum systems, in contrast to previous work with molecular H_2 [13].

Table 1. List of the test materials (Ma) and layer thicknesses in the Pd/Ma/Y layer stacks. The Pd layer was 4 nm for all samples. Values that differ from the rest are highlighted in bold.

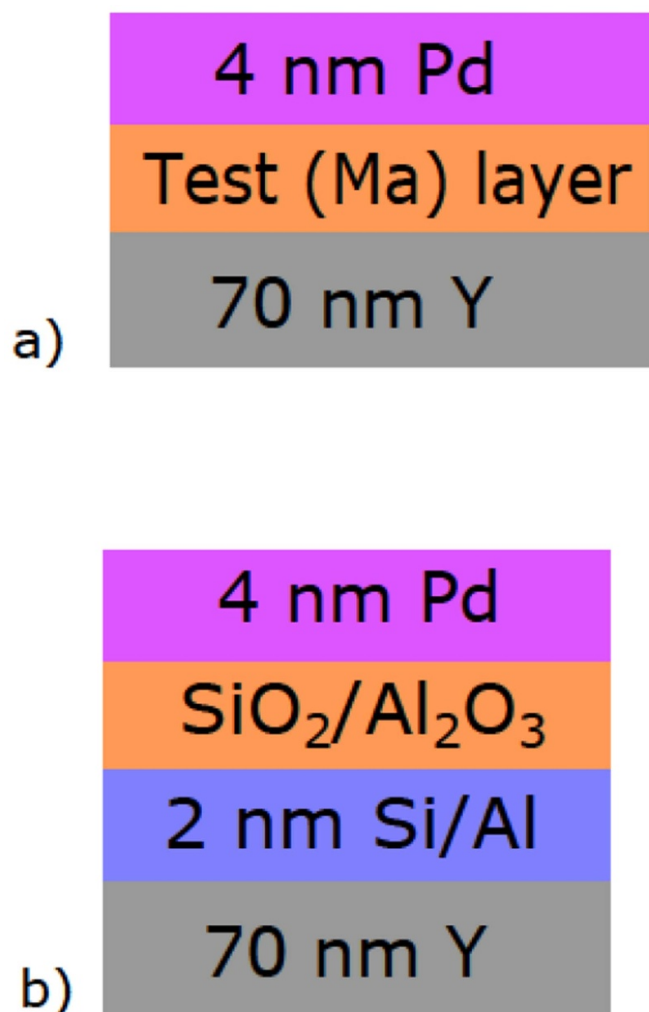| Material	Test layer — Thicknesses, nm	Y layer — Thickness, nm
Si	3, 6, 9, 12	70
Al	3, 6, 9, 12	70
Ag	3, 6, 9, 12	70
Ru	**5, 7**, 9, 12	70
Mo	3, 6, 9, 12	**80**
Cu	3, 6, 9, 12	70
SiO_2	3, 6, 9, 12	70
Al_2O_3	3, 6, 9, 12	70

Figure 1. Sketch of the sample structure (a) with metal or Si test layer and (b) with oxide test layer (additional thin metal layer is added for protection of the Y film from oxidation).

3. Experimental

For this study, pre-cut 15×15 mm^2 Si(001) wafer pieces were coated with thin films using DC magnetron sputtering, with the substrate held at room temperature. Deposition rates were calibrated with the aid of thickness measurements by Cu K$_\alpha$ x-ray reflection measurements. In combination with long term reproducibility of deposition rates, this leads to thickness errors of about 2% of the deposited film thickness. The film stacks consisted of a Y sensing layer, a test layer (Ma), and a Pd capping layer, which promotes hydrogen absorption (see figure 1(a) and table 1). The consecutive layers were deposited without breaking vacuum. Four sets of samples with test layer thicknesses between 3–12 nm (see table 1) were made for each material type. The oxide test layers Al_2O_3 and SiO_2 were reactively sputtered in Ar/O$_2$ plasma. Prior to reactive deposition of the oxide film, 2 nm Al (or Si in case of SiO_2) layer was deposited on the Y film to prevent Y oxidation by exposure to reactive O species in the plasma (see figure 1(b)). The stoichiometry of the oxides and purity of the Y layer

were confirmed with x-ray photoelectron spectroscopy (XPS, Thermo Fisher) after deposition. The roughness of the samples is dominated by the roughness of the 70 nm Y film. Typical samples show a 0.6 nm root mean square roughness measured in a 1×1 μm^2 atomic force microscopy image [11].

For exposures to H·, the samples were moved in air to a vacuum chamber with a base pressure of 2×10^{-8} mbar. Atomic hydrogen was generated by flowing 100 sccm H$_2$ gas over a tungsten filament heated to 2000°C, which was confirmed by measuring the temperature with an infrared temperature sensor (Raytek, RayMR1SCCF). A spectroscopic ellipsometer (Woollam M-2000XI, spectral range 240–1600 nm) was mounted to the vacuum system at an incidence angle of approximately 75° with respect to the surface normal, illuminating the front side of the sample. This allowed the evolution of Y hydrogenation to be measured *in situ*. The hydrogen exposure was terminated when the ellipsometric angles stopped changing, which previous work had confirmed to correspond to a formed YH$_2$ phase [12]. Additionally, post-exposure x-Ray diffraction (XRD, Panalytical Empyrean) measurements were used to verify the presence of YH$_2$.

4. Results and discussion

Before comparing the diffusion of hydrogen through thin films of different materials, we first demonstrate results showing the relevance of the Pd capping layer and atomic hydrogen source used in this work. In prior diffusion experiments, where molecular H$_2$ was used as hydrogen source, Pd caps acted both as a catalyst for H$_2$ dissociation, and as a protective layer for avoiding oxide formation on Y [14]. In this work, the Pd cap ensures that the test layer is subjected to the same atomic hydrogen concentration. For comparison, the hydrogenation of a multilayer with and without a Pd capping layer (Pd/Ru/Y and Ru/Y) is shown in figure 2. The speed of hydrogenation is significantly faster indicating the importance of surface processes.

The influence of the surface is further illustrated in figure 3, where the speed of hydrogenation for molecular and atomic hydrogen fluxes are compared. Atomic hydrogen clearly allows for much faster hydrogenation due to the elimination
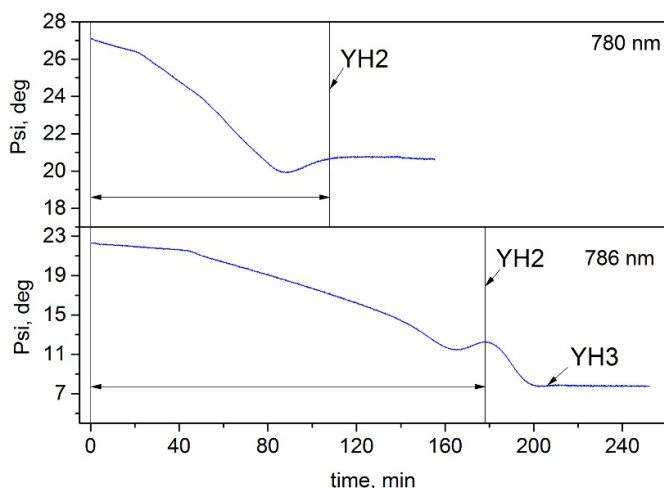
J. Phys. D: Appl. Phys. **53** (2020) 385302

O Soroka *et al*

Figure 2. Ellipsometry monitoring of hydrogenation with and without a Pd capping layer. In the presence of a Pd cap, the hydrogenation of Y saturates at the YH_2 phase (top), while a Ru/Y bilayer hydrogenates to a higher hydride, YH_3 (bottom).

of the dissociation process and the increase in the sticking coefficient.

The Pd/Ma/Y structured samples were exposed to atomic hydrogen until the Y layer was saturated and YH_2 formed. Formation of YH_2 is derived from saturation of the values of ellipsometry angles Ψ and Δ after a characteristic change as visible in figures 2 and 3 [11, 12]. It should be noted that the exact values of Ψ and Δ that correspond to YH_2 formation depend on the type of sample, since the ellipsometry signal is also influenced by the thicknesses and materials of other layers in the sample. Figure 4 shows the time taken to obtain the YH_2 phase for different Ma layer thicknesses. Note that the hydrogenation time for copper and molybdenum is, for the thickest layers, more than two orders of magnitude faster than for the remaining materials. Furthermore, both Si and Al samples could only be hydrogenated for layers up to 6 nm thick in the time allowed for the experiment (up to 10 d of continuous exposure, limited by the lifetime of the W filament). When the hydrogen exposure was started, changes in the ellipsometric angles Ψ and Δ due to Y lattice expansion [12] (similar to the first 40 min of exposure in the bottom graph in figure 2), were immediately apparent on all non-oxide samples, even for samples with slow hydrogenation, such as those with 6 nm Si or Al. The Al_2O_3 and SiO_2 oxide layers, on the contrary, showed no evidence that hydrogenation of the Y film had started after exposure to atomic hydrogen for times 195 h and 141 h, respectively (indicated with dotted lines). This was confirmed later with XRD measurements of the exposed samples, which found diffraction peaks for the Y phase only and no evidence of YH_2 formation.

There is no increase of the hydrogenation time for thicker Cu layers (figure 4). This indicates that Cu is not a limiting factor for hydrogen transport through the layered stack. It is interesting to note that the hydrogenation time actually decreases for a Cu thickness larger than 3 nm. It may be that alloying of Pd and Cu influences the hydrogenation speed [20]. The 3 nm Cu layer has a thinner interface with Pd and,

consequently, forms a Pd-Cu alloy with a higher Pd content. For the thicker Cu layers, the thickness of the interface is likely to be the same, though it is thicker than for the 3 nm Cu layer. This results in a higher concentration of Cu in the Pd-Cu alloy, which leads to a higher H diffusivity and smaller measured times [20].

It is likely that the hydrogen transport for 3 nm thick test layers of Al and Si is much faster compared to 6 nm thick layers because the 3 nm thick films do not form a closed layer. The failure to form a closed layer may be due to intermixing with Y or surface segregation of Y [21]. This results in pinholes forming, allowing direct contact between Pd and Y, which creates faster pathways for hydrogen transport compared to the pathway through the test layer.

The measured hydrogenation time grows with the thickness of the layer for all test layers except Cu. The times only reflect the accumulation of hydrogen in the Y sensor layer, which may be limited by a number of processes, including H adsorption on the Pd surface, surface-to-bulk transport at the Pd surface, diffusion in Pd, Y and, of course, diffusion through the test layer. When the measured hydrogenation time increases for thicker test layers, this indicates that the H permeability through the test layer has considerable impact on the overall hydrogenation kinetics. On the other hand, when the hydrogenation time is independent of, or do not increase with, test layer thickness, as in case of Cu, H permeates through the test layer much faster compared to the other processes. Therefore, we exclude Cu containing samples from the following analysis. Instead, Cu hydrogenation times are used as a limiting case to estimate the influence of surface processes on hydrogenation kinetics.

As prior research shows [22], hydrogen uptake in the Pd/Y system is limited by surface processes. The use of H· accelerates H uptake significantly, but the hydrogenation still takes several minutes in the conditions of our experiment. Taking into account the diffusion coefficients of hydrogen in Pd and Y at room temperature (shown in table 2) a diffusion model as described in previous work (see [13] and further explanation in this paper) can be used to estimate the diffusion time through Pd and Y layers [13, 23]. Using this model, the time that is needed to obtain the required hydrogen fluence for YH_2 saturation through 4 nm Pd and 70 nm of Y would be about 0.01 and 0.21 s, respectively. Since this is few orders of magnitude faster than the observed hydrogenation time, this confirms our assumption that the uptake is limited by surface processes in the case of a Cu test layer.

In order to evaluate the relative speed of diffusion through the different test materials, we now focus on measured hydrogenation times for 6 nm test layers, since, for that thickness, saturation to YH_2 could be reached for all non-oxide test materials, while artefacts due to pinholes are expected to be absent. In figure 5, these hydrogenation times are compared to the heat of solution of H in the test material, where a lower heat of solution indicates that it is thermodynamically more favorable to dissolve hydrogen in the material. Though the mechanism of the hydrogen transport may vary from one material to another, the apparent hydrogenation time (which is inversely proportional to the diffusion constant) exponentially scales with the heat of H solution. This suggests that the heat of H
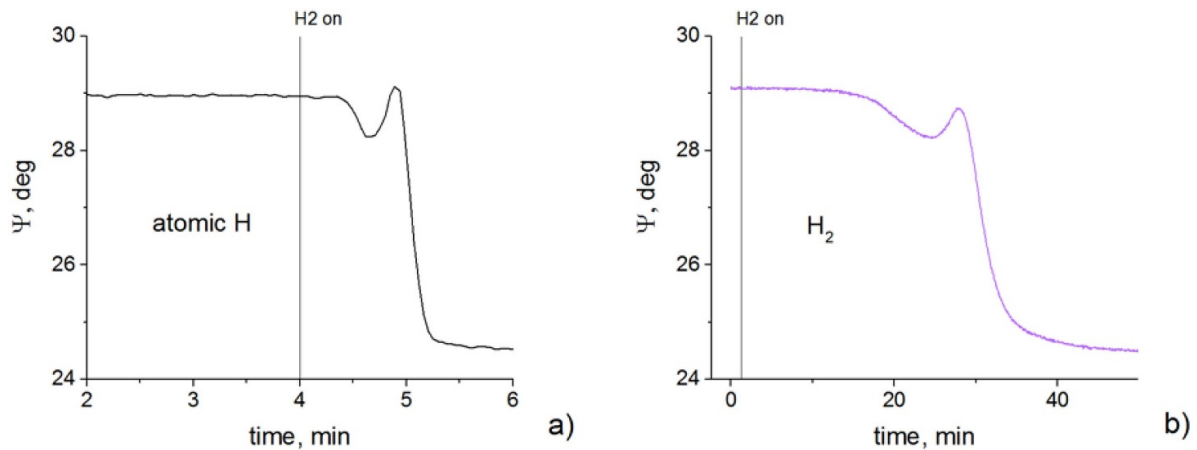
Figure 3. Ellipsometry monitoring (at wavelength 1111.9 nm) of hydrogenation of a Pd/Y bilayer with (a) atomic hydrogen (generated with W filament) with a H_2 flow of 100 sccm and (b) with only molecular hydrogen of 200 sccm flow. For atomic hydrogen exposure the filament was switched on before introducing hydrogen to the chamber. The vertical line 'H2 on' marks the time at which hydrogen is admitted in the chamber.
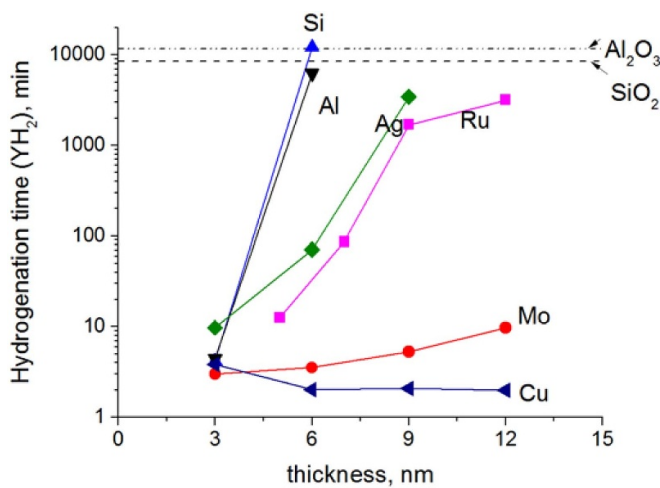

Figure 4. Time required for YH_2 formation for different test layers (Cu, Mo, Ru, Ag, Al, and Si) depending on the thickness of the test layer. The hydrogen flow was set to 100 sccm for all test layers except for Mo, where it was reduced to 26 sccm in order to prevent that hydrogenation would be faster than the time resolution of ellipsometry monitoring. No measurable hydrogenation was observed for 3 and 6 nm thick Al_2O_3 and SiO_2 test layers in the indicated times.

solution can serve as an initial reference parameter for estimating the hydrogen transport rate through thin films. It should be noted that, to our knowledge, there is no theoretical explanation available in literature that relates hydrogen diffusion with heat of solution in a material.

For Ru, Ag, Al and Si the hydrogenation time increases much faster with layer thickness compared to Mo, where the results follow a linear diffusion model described earlier [13]. We speculate that for polycrystalline materials (Ru, Al and Ag), where the hydrogen solubility is low compared to Mo, defects and grain boundaries are the main pathway for hydrogen diffusion. Since the grain structure (and possibly also the defect density) is expected to change as a function of film

thickness, the hydrogen permeability of the test material can be expected to depend on film thickness. Si, on the other hand, forms a non-crystalline amorphous layer, which eliminates grain boundary diffusion, making the influence of defects more significant. Defects in amorphous silicon are known to trap hydrogen and, consequently, should increase the hydrogenation time [33].

When the test layer limits hydrogen uptake, a concentration gradient of hydrogen forms across the test layer. In the case of thin layers, the steady state regime of diffusion is reached much faster than the H loading time. Therefore, the concentration gradient can be assumed linear and time-independent during the entire hydrogenation process, as was previously shown by Borgschulte and Gremaud [23]. Assuming that hydrogen uptake is limited by diffusion through the test layer (via grain boundaries or bulk), the hydrogenation rates should scale linearly with the diffusion constant of the test layer. To test this, the hydrogenation times were calculated with a simplified model (described in detail in [13]) for hydrogen diffusion through a layered stack [13]. According to Fick's second law, the change in hydrogen concentration, C, with respect to time, t, in the test layer can be expressed as a function of the diffusion constant, D, and depth, z, in the test layer:

$$\frac{\partial C}{\partial t} = D \frac{\partial^2 C}{\partial z^2}. \tag{1}$$

The model takes into account H diffusion in the test layer resulting from a fixed concentration at the boundaries, assuming the concentrations at the Pd/Ma and Ma/Y interfaces to be C_{Pd} (justified by the rapid absorption in Pd compared to diffusion through the test layer) and zero, respectively (see figure 6(a)). At the Ma/Y interface, the negative enthalpy of formation of YH_2 (compared to positive enthalpy of formation for the test materials) ensures that Y acts as a sink for H, such that the concentration can be assumed to be close to zero [13]. The hydrogen flux at Ma/Y interface is calculated using the diffusion equation (1). The total number of hydrogen atoms

Table 2. Literature values of heat of solution and diffusion coefficient of hydrogen at room temperature for test materials, Pd and Y. Specimen type and method of measuring diffusion constant are indicated for literature data, including reference.

| Material	Crystal structure	Heat of solution of hydrogen, eV/atom [24]	Diffusion constant range from this study, m^2/s	Reported diffusion constant at room temperature, m^2/s	Reference
Mo	bcc	0.259	1.48×10^{-18}–2.63×10^{-18}	1.9×10^{-23}	7 mm thick foil, electromigration [25]
				2.1×10^{-17}	Tube, permeation through tube walls [26]
				2.2×10^{-13}	Spherical single crystal, thermal outgassing [27]
Cu	fcc	0.476			
				1.1×10^{-14}	[28]
Ru	hcp	0.559	5.7×10^{-21}–5.9×10^{-19}	1.9×10^{-19}	nm thick film, hydrogenography [13]
Al	fcc	0.621	1.4×10^{-21}–1.23×10^{-18}	2.6×10^{-11}	2 mm thick wire, desorption; [29]
				5.2×10^{-22}	10 mm block, desorption [29]
				5.3×10^{-12}	μm thick thick membrane, permeation [30]
Ag	fcc	0.652	3.9×10^{-21}–4.5×10^{-19}		
				1.9×10^{-13}	[28]
Si	fcc	1.865	7.4×10^{-22}–1.31×10^{-18}	1.1×10^{-23}	μm thick film of poly-Si, SIMS [31]
				2.2×10^{-32}	a-Si, H-D interdiffusion [32]
Pd	fcc	−0.103		1.9×10^{-15}	nm thick films, electrochemical stripping technique [19]
Y	hcp	−0.818		3×10^{-14}	nm thick films, hydrogenography [22]
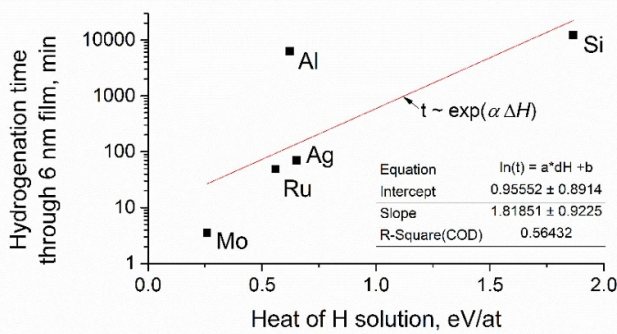
Figure 5. Hydrogenation time for layer stacks with 6 nm films of test material versus the heat of solution of hydrogen in test materials (note the logarithmic scale). The time scales with the heat of solution exponentially. The fitted line is proportional to $\exp(\alpha \Delta H)$, with α a constant.

accumulated in Y film can be then obtained by integrating the calculated hydrogen flux over the exposure time. This allows the hydrogenation time of the Y film to be estimated as a function of the thickness of the test layer. The calculation results for three different diffusion coefficients are presented in figure 6(b). A higher diffusion coefficient leads to faster hydrogenation, however, the slope of time versus test layer thickness in a semilogarithmic plot remains the same. The effect of a changing diffusion constant is a vertical offset. The best fit for Mo samples is shown along with the measured data. The data for the other test layers cannot be fit by a single diffusion constant for the material, implying that the mechanisms of the hydrogen diffusion depends on film thickness. Thus, the hydrogenation rates of thin-films in the range of 3–12 nm cannot be predicted by a diffusion model using only a single diffusion constant. This is in line with a prior study of Pasturel *et al* [34], where

the measured hydrogen uptake by a Mg_2Ni hydrogen sensitive layer did not depend in a straightforward way on the diffusivity in test metal layers. These results suggest that the diffusion constant of hydrogen through the test layers depends on layer structure and thickness, as discussed above. In addition, the solubility and film structure have a stronger influence on the hydrogen concentration gradient than included in our model.

Using the described model, effective diffusion coefficients were calculated for each measurement point in figure 4, (excluding Cu). The ranges of the obtained diffusion coefficients are shown in table 2.

When comparing the diffusion coefficients obtained in this work to the values from literature for materials used in this study (see table 2), a few interesting observations can be made. The obtained coefficients for Ru samples agree with the value from the previous study, which used Ru films deposited in the same conditions as in this work. On the contrary, literature values for H diffusion in Ag are six orders of magnitude higher than the range of the calculated values, which is likely caused by the difference in sample microstructure.

Al presents an interesting case. Previous studies show a 13 order of magnitude spread in reported H diffusion constants, which is likely caused by different diffusion pathways (bulk, vacancies, or defects) dominating for samples investigated in different conditions [29]. According to table 2, the largest reported diffusion constant for Al is higher than for Pd and Y, meaning that the results for Al should be similar to those of Cu. However, the calculated diffusion coefficient for Al in this work is in line with those of the smaller diffusion constants found in the literature (see table 2). Our results add to the body of evidence that suggests that the effective diffusion rate in Al is extremely sensitive to experimental conditions, including film deposition parameters. The relatively low heat of solution predicts fast diffusion processes (see
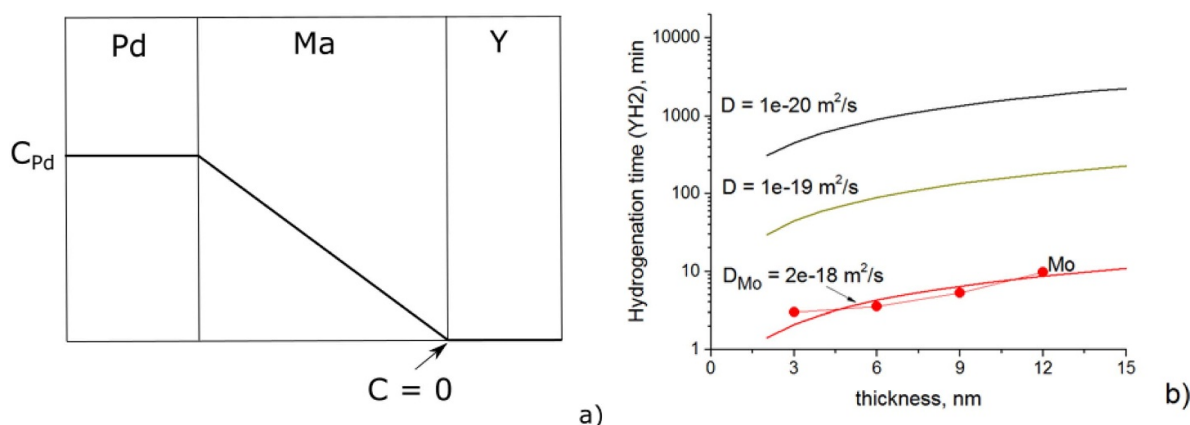
J. Phys. D: Appl. Phys. **53** (2020) 385302

O Soroka *et al*

Figure 6. (a) A sketch of the hydrogen concentration profile assumed in the diffusion model. (b) Calculated hydrogenation times as a function of the layer thickness for three values of the diffusion coefficient of hydrogen in the test layer. The best fit for the Mo measured data is shown.

figure 5), in agreement with larger diffusion constants. However, as discussed in [29], it is possible that a large density of defects or vacancies increases the measured hydrogenation time.

A wide spread of reported diffusion coefficients is also observed for Mo and Si (table 2). This, combined with the (large) qualitative differences in hydrogen diffusion between our experiment and literature values of hydrogen diffusion, may be related to different methods used for probing diffusion, the different form of materials (thin films, powders or bulk materials), and, for thin-films, different deposition conditions, used for those studies. This stresses the importance that the measurement of diffusion constants or comparison of hydrogen diffusion properties should be performed with materials fabricated using similar methods, and identical methods for probing hydrogen diffusion should be used.

5. Summary and conclusions

In this work, we demonstrated a method for measuring hydrogen permeation through nanometer range thin films of Si, Al, Ag, Ru, Mo, Cu, SiO_2 and Al_2O_3 deposited on top of a Y film that acts as sensor layer. Ellipsometry was used to monitor the transition of the Y film to YH_2, in order to extract the relative rate of hydrogen diffusion through the test films as function of material and thickness. All samples had a protective Pd capping layer that ensures that all test materials were exposed to the same concentration of H dissolved in Pd at the Pd/test material interface.

No hydrogen diffusion through SiO_2 and Al_2O_3 could be observed for the conditions and accessible time scales of this work. This indicates that oxides in general are better barriers for hydrogen diffusion compared to elemental materials, which is in agreement with prior studies using molecular hydrogen [35, 36]. It was shown earlier [37] that hydrogen diffusivity in oxides proceeds via hydrogen jumping between neighboring oxygen atoms and relies on dynamics of the host oxide atoms. Close packed oxides

(like Al_2O_3 and SiO_2) do not allow a high degree of O-atom movement and, hence, act as an efficient hydrogen barrier.

We observed that for all metals, except Cu, the hydrogenation rate of Y was limited by H diffusion through the test material. The hydrogenation time roughly scales with the heat of solution of H in the test material, indicating that heat of solution can serve as a first indicator for H diffusion speed through a material. The calculated diffusion constants are within the range of diffusion constant values reported in literature, with the exception of that of Ag. However, the range of values also indicates the importance of systematic effects due to differences in measurement methods and material preparation. This stresses the importance that H diffusion properties should be measured in a sample structure that is directly relevant for the application for which H diffusion properties are to be determined. Nevertheless, the proposed sensor is a valuable tool when the evaluation of the hydrogen diffusion is needed for test layers at hand.

ORCID iD

J M Sturm https://orcid.org/0000-0002-0731-6329

J. Phys. D: Appl. Phys. **53** (2020) 385302

O Soroka *et al*

References

[1] Kirchheim R and Pundt A 2014 Hydrogen in metals *Physical Metallurgy* 5th edn (Amsterdam: Elsevier)

[2] Horinouchi H, Shinohara M, Otsuka T, Hashizume K and Tanabe T 2013 Determination of hydrogen diffusion and permeation coefficients in pure copper at near room temperature by means of tritium tracer techniques *J. Alloys Compd.* **580** S73

[3] Mézin A, Lepage J and Abel P B 1996 Hydrogen permeation properties of molybdenum coatings from absorption-desorption experiments *Thin Solid Films* **272** 132–6

[4] Gremaud R, Broedersz C P, Borsa D M, Borgschulte A, Mauron P, Schreuders H, Rector J H, Dam B and Griessen R 2007 Hydrogenography: an optical combinatorial method to find new light-weight hydrogen-storage materials *Adv. Mater.* **19** 2813–7

[5] Nemanič V 2019 Hydrogen permeation barriers: basic requirements, materials selection, deposition methods, and quality evaluation *Nucl. Mater. Energy* **19** 451–7

[6] Graham S, Steinhaus C, Clift M and Klebanoff L 2002 Radio-frequency discharge cleaning of silicon-capped Mo/Si multilayer extreme ultraviolet optics *J. Vac. Sci. Technol.* B **20** 2393–400

[7] van den Bos R 2018 *Hydrogen Infuced Blister Formation in Mo/Si Multilayer Structures* (Enschede: University of Twente)

[8] Dwivedi S K and Vishwakarma M 2018 Hydrogen embrittlement in different materials: a review *Int. J. Hydrogen Energy* **43** 21603–16

[9] Van Den Bos R A J M, Lee C J, Benschop J P H and Bijkerk F 2017 Blister formation in Mo/Si multilayered structures induced by hydrogen ions *J. Phys. D: Appl. Phys.* **50** 265302

[10] Hübert T, Boon-Brett L, Black G and Banach U 2011 Hydrogen sensors—review *Sensors Actuators* B **157** 329–52

[11] Soroka O, Sturm J M, van de Kruijs R W E, Lee C J and Bijkerk F 2018 Control of YH$_3$ formation and stability via hydrogen surface adsorption and desorption *Appl. Surf. Sci.* **455** 70–4

[12] Soroka O, Sturm J M, van de Kruijs R W E, Makhotkin I A, Nikolaev K, Yakunin S N, Lee C J and Bijkerk F 2019 Hydrogenation dynamics of Ru capped Y thin films *J. Phys. D: Appl. Phys.* **126** 145301

[13] Soroka O, Sturm J M, Lee C J, Schreuders H, Dam B and Bijkerk F 2020 Hydrogen diffusion through Ru thin films *Int. J. Hydrogen Energy* **45** 15003

[14] Den Broeder F J A *et al* 1998 Visualization of hydrogen migration in solids using switchable mirrors *Nature* **394** 656–8

[15] Remhof A, Van Der Molen S J, Antosik A, Dobrowolska A, Koeman N J and Griessen R 2002 Switchable mirrors for visualization and control of hydrogen diffusion in transition metals *Phys. Rev.* B **66** 020101

[16] Schweppe F, Martin M and Fromm E 1997 Model on hydride formation describing surface control, diffusion control and transition regions *J. Alloys Compd.* **261** 254–8

[17] Borgschulte A, Westerwaal R J, Rector J H, Schreuders H, Dam B and Griessen R 2006 Catalytic activity of noble metals promoting hydrogen uptake *J. Catal.* **239** 263–71

[18] Ngene P, Radeva T, Slaman M, Westerwaal R J, Schreuders H and Dam B 2014 Seeing hydrogen in colors: low-cost and highly sensitive eye readable hydrogen detectors *Adv. Funct. Mater.* **24** 2374–82

[19] Li Y and Cheng Y T 1996 Hydrogen diffusion and solubility in palladium thin films *Int. J. Hydrog. Energy* **21** 281–91

[20] Westerwaal R J, Bouman E A, Haije W G, Schreuders H, Dutta S, Wu M Y, Boelsma C, Ngene P, Basak S and Dam B 2015 The hydrogen permeability of Pd-Cu based thin film membranes in relation to their structure: a combinatorial approach *Int. J. Hydrog. Energy* **40** 3932–43

[21] Chandrasekaran A, Van de Kruijs R W E, Sturm J M, Zameshin A A and Bijkerk F 2019 Nanoscale transition metal thin films: growth characteristics and scaling law for interlayer formation *ACS Appl. Mater. Interfaces* **11** 46311–26

[22] Borgschulte A, Lohstroh W, Westerwaal R J, Schreuders H, Rector J H, Dam B and Griessen R 2005 Combinatorial method for the development of a catalyst promoting hydrogen uptake *J. Alloys Compd.* **404–6** 699–705

[23] Borgschulte A, Gremaud R and Griessen R 2008 Interplay of diffusion and dissociation mechanisms during hydrogen absorption in metals *Phys. Rev.* B **78** 094106

[24] Griessen R and Riesterer T 1988 Heat of formation models *Hydrog. Intermet. Compd. Electron. Hydrogen in Intermetallic Compounds I (Topics in Applied Physics)* vol 63 (Berlin: Springer)

[25] Pietrzak R and Rozenfeld B 1990 The electromigration and diffusion of hydrogen in molybdenum *J. Less-Common Met.* **162** 23–31

[26] Zakharov A P, Sharapov V M and Evko E I 1975 Hydrogen permeability of polycrystalline and monocrystalline molybdenum and tungsten *Sov. Mater. Sci.* **9** 149–53

[27] Katz L, Guinan M and Borg R J 1971 Diffusion of H$_2$, D$_2$, and T$_2$ in single-crystal Ni and Cu *Phys. Rev.* B **4** 330–41

[28] Verbetsky V N and Mitrokhin S V 2000 Copper- silver- and gold-hydrogen *Solid State Phenom.* **73–75** 503

[29] Young G A and Scully J R 1998 The diffusion and trapping of hydrogen in high purity aluminum *Acta Mater.* **46** 6337–49

[30] Katsuta H and McLellan B R 1979 Diffusivity of hydrogen in silver *Scr. Metall.* **13** 65–66

[31] Jackson W B, Johnson N M, Tsai C C, Wu I - W, Chiang A and Smith D 1992 Hydrogen diffusion in polycrystalline silicon thin films *Appl. Phys. Lett.* **61** 1670–2

[32] Carlson D E and Magee C W 1978 A SIMS analysis of deuterium diffusion in hydrogenated amorphous silicon *Appl. Phys. Lett.* **33** 81–3

[33] Peeters F J J, Zheng J, Aarts I M P, Pipino A C R, Kessels W M M and van de Sanden M C M 2017 Atomic hydrogen induced defect kinetics in amorphous silicon *J. Vac. Sci. Technol.* A **35** 05C307

[34] Pasturel M, Wijngaarden R J, Lohstroh W, Schreuders H, Slaman M, Dam B and Griessen R 2007 Influence of the chemical potential on the hydrogen sorption kinetics of Mg 2 Ni/TM/Pd (TM = transition metal) trilayers *Chem. Mater.* **19** 624–33

[35] Earwaker L G, Ross D K, Farr J P G and Cheetham J L 1981 The influence on hydrogen premeation through steel of surface oxide layers and their characterisation using nuclear reactions *IEEE Trans. Nucl. Sci.* **28** 1848–50

[36] Fromm E and Uchida H 1987 Surface phenomena in hydrogen absorption kinetics of metals and intermetallic compounds *J. Less Common Met.* **131** 1–12

[37] Norby T, Widerøe M, Glöckner R and Larring Y 2004 Hydrogen in oxides *Dalt. Trans.* **2004** 3012–8